How to optically count graphene layers

Sosan Cheon,[1] Kenneth David Kihm,[1,2,*] Jae Sung Park,[1] JoonSik Lee,[1] Byeong Jun Lee,[3] Hyeoungkeun Kim,[4] and Byung Hee Hong[5]

[1]*World Class University Program, Seoul National University, Seoul 151-744, South Korea*

[2]*Mechanical, Aerospace, and Biomedical Engineering, The University of Tennessee, Knoxville, Tennessee 37996, USA*

[3]*Mechanical Engineering, Yeungnam University, Gyeongsan, Gyeongbuk 712-749, South Korea*

[4]*Electronic Materials and Device Research Center, Korea Electronics Technology Institute, Seongnam 463-816, South Korea*

[5]*Department of Chemistry, Seoul National University, Seoul 151-742, South Korea*

**Corresponding author: kkihm@utk.edu*

Received July 6, 2012; revised July 30, 2012; accepted July 30, 2012;
posted July 30, 2012 (Doc. ID 172014); published 0 MONTH 0000

The total thickness of a graphene sample depends upon the number of individually stacked graphene layers. The corresponding surface plasmon resonance (SPR) reflectance alters the SPR angle, depending on the number of graphene layers. Thus, the correlation between the SPR angle shift and the number of graphene layers allows for a nonintrusive, real-time, and reliable counting of graphene layers. A single-layer graphene (SLG) is synthesized by means of chemical vapor deposition, followed by physical transfer to a thin gold film (48 nm) repeatedly, so that multilayer graphene samples with one, three, and five layers can be prepared. Both the measured SPR angles and the entire reflectance curve profiles successfully distinguish the number of graphene layers. © 2012 Optical Society of America

OCIS codes: 310.0310, 240.0240.

Graphene, a two-dimensional(2D) sheet of carbon atoms, has drawn significant interest from both the scientific and engineering fields because of its novel electrical, thermal, and mechanical properties [1–5]. While single-layer graphene(SLG) provides a 2D structure of 0.335 nm thickness, the reliable counting of graphene layers is essential to define the properties of multilayer graphene (MLG) [6,7]. To date, several optical counting methods have been attempted; however, none has proven to be robust and reliable. Our new method of counting graphene layers by detecting the surface plasmon resonance (SPR) angle shifts has turned out to be not only highly repeatable but also accurate, overcoming the limitations of these previous attempts to count graphene layers.

Various efforts to count graphene layers by observing the Raman spectra [8–12] have been relatively well exploited but remain under controversy because of such factors as the extrinsic effects of any impurities, defects, crystallinity, and optical configurations of the substrate [12,13], as well as the uncertainties of 2D band deconvolution [14]. Furthermore, the consistent dependence of the Raman spectrum on the number of layers requires Bernal-stacked atomic layers (coincident hexagonal carbon structures) such as the exfoliated graphene. The chemical vapor deposition (CVD) method is considered to be a more practical way to obtain graphene, particularly graphene of larger size and high throughput, but it is implausible to apply the Raman method to MLGs by CVD with randomly oriented layers, which inevitably result from the mechanical stacking of SLGs to construct MLG samples [15–18].

Another previous attempt, atomic force microscopy (AFM), measures the thickness of an MLG when the SLG thickness is known [19]. However, the unknown gap thickness between adjacent layers causes inherent uncertainties for this technique. Use of various microscopic techniques allows for a clearer distinction of SLG from MLG but fails to count graphene layers [20]. On the other hand, optical reflectance detection [21] is limited in qualitatively distinguishing graphene samples with different layers only when the staggered graphene layer edges are exposed. More recently, a spectral theory of optical reflectance from SLG and MLG has been developed using dynamic conductivity modeling [22], but no experimental work has been conducted to use this to count graphene layers.

In order to develop a more robust counting and quantitative scheme, what we propose herein is to use the SPR reflectance involving the SPR angle dependence

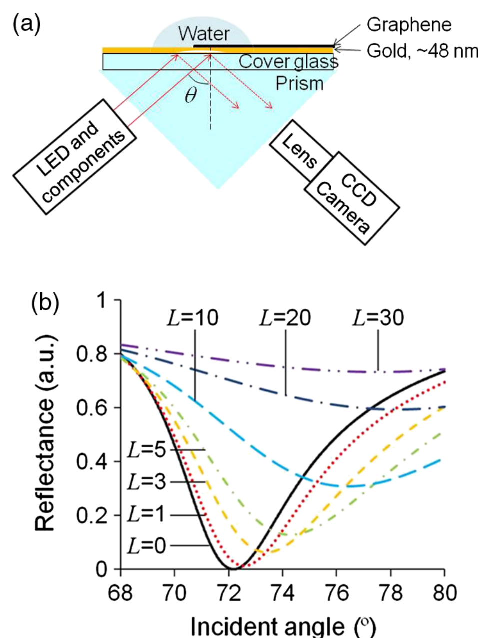

Fig. 1. (Color online) (a) The SPR reflectance imaging layout, and (b) the calculated SPR reflectance curves [Eq. (1)] as functions of the number of graphene layers (L), using a dielectric constant $\varepsilon = -11.65 - 1.271i$ for the gold film [32] and 6.19–$8.64i$ for graphene [26] at 634 nm wavelength.

0146-9592/12/180001-01$15.00/0 © 2012 Optical Society of America

to accurately count the number of graphene layers. Our laboratory-assembled SPR layout [23], which is based on Kretschtmann's configuration [24] [Fig. 1(a)], enables us to observe a significant reduction in the reflection intensity from the total internal reflectance level by the resonant coupling of the evanescent wave field imposed upon the free electrons in the thin metal film (Au). The incident angle for the resonance is called the SPR angle, which turns out to be the most sensitive and robust discrimination for graphene counting. Note that the magnitudes of reflectance are affected by the optical alignment and/or background light nonuniformities [25], and that the spectroscopic analysis requires a reliable dispersion relation for graphene [26,27].

A formula for the reflectance from a four-layer system is required to know the theoretical SPR angle [28]:

$$R = \frac{r_1[1+\exp(-2ik_2d_2)] + [r_1r_2 + \exp(-2ik_2d_2)]r_3\ \exp(-2ik_3d_3)}{1 + r_1r_2\ \exp(-2ik_2d_2) + [r_2 + r_1\ \exp(-2ik_2d_2)]r_3\ \exp(-2ik_2d_2)} \quad (1)$$

where r_i denotes the amplitude coefficient of reflection between the ith and $(i+1)$th layers and k_i represents the wave vector in each medium, with the subscript $i = 1,\ 2,\ 3,$ and 4 referring to the BK7 prism ($n = 1.515$), the gold film of thickness $d_2 = 48$ nm, the graphene layers of total thickness d_3(≡ number graphene layers $L \times$ SLG thickness of 0.335 nm, and water as the environmental medium above the graphene sample, respectively.

The water medium provides a larger SPR angle (72.1°) than that of the air (43.8°). This larger SPR angle ensures larger SPR angle shifts [25,29], which substantially enhances measurement accuracy when detecting the shift angles. Figure 1(b) shows calculated reflectance as functions of the incident angle. The dipped shapes of these curves predict clear distinctions for different numbers of layers, and the SPR angles show a consistent increase with increasing L. When the number of graphene layers exceeds 10, the SPR curve broadens and the definition of the SPR angle becomes less discriminating with the number of layers [Fig. 1(b)].

SLGsamples, synthesized via the CVD process using a copper foil substrate, were repeatedly transferred onto a gold surface to fabricate MLG samples of $L = 3$ and $L = 5$ [17,18]. The Raman spectra of the three samples show no prominent D peak (1340 cm^{-1}) (Fig. 2), indicating that the level of defects in our graphene samples is very low. Despite our repeated attempts, however, it was not possible to confirm a reliable Raman correlation with the number of layers. As aforementioned, the random stacking of CVD MLGs does not allow for consistent Raman correlation with the number of graphene layers, unlike theexfoliated MLGs from highly ordered pyrolytic graphite. The resulting Raman spectra for the MLGs look similar to those of the SLG except for the relatively enhanced intensities [15,16]. The intensity ratio of the G peak to the 2D peak (2680 cm^{-1}) also randomly varies with L, that is, $G/2D = 0.29$, 0.30, and 0.25 for $L = 1$, 3, and 5, respectively, without any consistency.

Under our new method, the SPR angle shift discriminations provide much more reliable and repeatable counting of the graphene layers (Fig. 3). Each symbol represents the measured reflectance intensity, which is spatially averaged over an area of $1.7 \times 10^3\ \mu\text{m}^2$ on the graphene surface, and the solid curves represent calculations based on the extended Fresnel theory of Eq. (1). All normalized SPR reflectance curves are presented in Fig. 3 so that the SPR angles can be more clearly distinguished, as the SPR reflectance magnitudes can bias with various experimental conditions.

Measurements were repeated for three different areas in a single sample in order to ensure the robustness of this method with respect to impurities and other graphene surface quality factors. The error bars represent

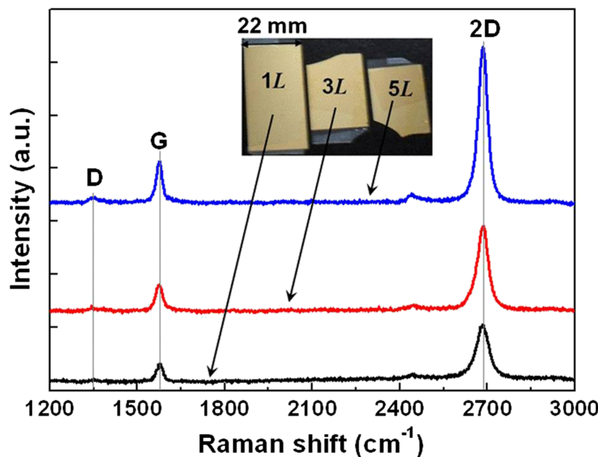

Fig. 2. (Color online) Raman spectra of one, three, and five-graphene layers on gold film. The locations of the G (1590 cm^{-1}) and 2D (2680 cm^{-1}) peaks of the SLG are marked with the two vertical lines.

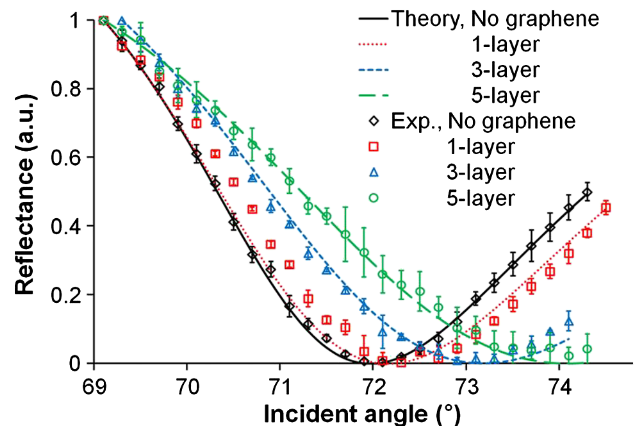

Fig. 3. (Color online) Measured and calculated [Eq. (1)] SPR reflectance variations with the incident angle for one, three, and five graphene layers laid on a 48 nm gold film (Fig. 1).

Table 1. Measured SPR Angles of Multilayer Graphenes and Calculated Values with Three Different Dielectric Constants

$\varepsilon_{\text{graphene}}$	$L = 0$	$L = 1$	$L = 3$	$L = 5$
	Measured SPR Angles			
	$71.9 \pm 0.1°$	$72.3 \pm 0.1°$	$73.0 \pm 0.1°$	$73.9 \pm 0.4°$
	Calculated SPR Angles			
$6.19–8.64i$ [26]	71.9°	72.2°	73.1°	73.9°
$7.04–8.40i$ [27]		72.3°	73.1°	74.0°
$2.79–4.40i$ [31]		72.1°	72.7°	73.3°

the maximum data fluctuation ranges for three independent realizations of each layer. The reflectance measurements without graphene were also repeated three times, ensuring measurement accuracy as well as consistency. The measured reflectance data show remarkable consistency and repeatability.

The MLG samples may develop thin gaps of an order of 1 nm [30] between graphene layers as a result of the layer-by-layer transfer of SLGs, but the reflectance should not be significantly altered by the gap because the reflectance is almost entirely determined by the pi-electrons in the graphene layers.

Table 1 shows the dependence of the SPR angle predictions on the number of graphene layers for three different choices of dielectric constants of graphene. Our measured SPR angles turned out to best agree with the calculations using the dielectric constant predicted by the density functional theory (DFT) [26]. The measured dielectric constant using picometrology [27] provided almost identical results to the case using the DFT, within the angle detection uncertainty of $\pm 0.1°$ of the digital protractor Model Pro3600 of SMARTTOOL. In contrast, the SPR angles using the spectroscopically determined dielectric constant [31] noticeably deviated from the measured data; this may be attributed to the imposed assumption of a dielectric constant independent of the incident wavelength.

In summary, the number of CVD graphene layers was optically determined based on the SPR angle shifts associated with increasing numbers of graphene layers. This method seems to be far more consistent and repeatable than any of the previous attempts, including Raman spectroscopy, the relative reflectance or transmittance variations, microscopic imaging techniques, and AFM. Furthermore, the reflectance calculations using Fresnel's equations provide theoretical support to the SPR method by showing excellent agreement with the measured SPR angles.

This research work was supported partially by the World Class University (WCU) Program (R31-2008-000-10083-0) and partially by the Nano-Material Technology Development Program (R2011-003-2009), both through the National Research Foundation of Korea (NRF) funded by the Ministry of Education, Science and Technology.

References

1. A. K. Geim and K. S. Novoselov, Nat. Mater. **6**, 183 (2007).
2. A. K. Geim, Science **324**, 1530 (2009).
3. C. Lee, X. Wei, J. W. Kysar, and J. Hone, Science **321**, 385 (2008).
4. K. S. Kim, Y. Zhao, H. Jang, S. Y. Lee, J. M. Kim, K. S. Kim, J.-H. Ahn, P. Kim, J.-Y. Choi, and B. H. Hong, Nature **457**, 706 (2009).
5. Y.-M. Lin, K. A. Jenkins, A. Valdes-Garcia, J. P. Small, D. B. Farmer, and P. Avouris, Nano Lett. **9**, 422 (2008).
6. Y. Sui and J. Appenzeller, Nano Lett. **9**, 2973 (2009).
7. P. Gava, M. Lazzeri, A. M. Saitta, and F. Mauri, Phys. Rev. B **79**, 165431 (2009).
8. D. Graf, F. Molitor, K. Ensslin, C. Stampfer, A. Jungen, C. Hierold, and L. Wirtz, Nano Lett. **7**, 238 (2007).
9. A. C. Ferrari, J. C. Meyer, V. Scardaci, C. Casiraghi, M. Lazzeri, F. Mauri, S. Piscanec, D. Jiang, K. S. Novoselov, S. Roth, and A. K. Geim, Phys. Rev. Lett. **97**, 187401 (2006).
10. I. Calizo, W. Z. Bao, F. Miao, C. N. Lau, and A. A. Balandin, Appl. Phys. Lett. **91**, 201904 (2007).
11. A. Gupta, G. Chen, P. Joshi, S. Tadigadapa, and Eklund, Nano Lett. **6**, 2667 (2006).
12. D. Yoon, H. Moon, Y.-W. Son, J. S. Choi, B. H. Park, Y. H. Cha, Y. D. Kim, and H. Cheong, Phys. Rev. B **80**, 125422 (2009).
13. C. Casiraghi, S. Pisana, K. S. Novoselov, A. K. Geim, and A. C. Ferrari, Appl. Phys. Lett. **91**, 233108 (2007).
14. L. M. Malard, M. H. D. Guimaraes, D. L. Mafra, M. S. C. Mazzoni, and A. Jorio, Phys. Rev. B **79**, 125426 (2009).
15. J. Hass, F. Varchon, J. E. Millán-Otoya, M. Sprinkle, N. Sharma, W. A. de Heer, C. Berger, P. N. First, L. Magaud, and E. H. Conrad, Phys. Rev. Lett. **100**, 125504 (2008).
16. Z. Ni, Y. Wang, T. Yu, Y. You, and Z. Shen, Phys. Rev. B **77**, 235403 (2008).
17. X. Li, Y. Zhu, W. Cai, M. Borysiak, B. Han, D. Chen, R. D. Piner, L. Colombo, and R. S. Ruoff, Nano Lett. **9**, 4359 (2009).
18. J. Kang, H. Kim, K. S. Kim, S.-K. Lee, S. Bae, J.-H. Ahn, Y.-J. Kim, J.-B. Choi, and B. H. Hong, Nano Lett. **11**, 5154 (2011).
19. K. S. Novoselov, A. K. Geim, S. V. Morozov, D. Jiang, Y. Zhang, S. V. Dubonos, I. V. Grigorieva, and A. A. Firsov, Science **306**, 666 (2004).
20. K. D. Kihm, J. S. Park, S. S. Cheon, and J. S. Lee, J. Heat Transfer—Photogallery **133**, 080902 (2011).
21. P. Blake, E. W. Hill, A. H. C. Neto, K. S. Novoselov, D. Jiang, R. Yang, T. J. Booth, and A. K. Geim, Appl. Phys. Lett. **91**, 063124 (2007).
22. L. A. Falkovsky, J. Phys.: Conf. Ser. **129**, 012004 (2008).
23. K. D. Kihm, Exp. Fluids **48**(4), 547 (2010).
24. E. Kretschmann, Z. Physik. A Hadron Nuclei **241**, 313 (1971).
25. K. D. Kihm, S. Cheon, J. S. Park, H. J. Kim, J. S. Lee, I. T. Kim, and H. J. Yi, Opt. Las. Eng. **50**, 64 (2012).
26. M. Klintenberg, S. Lebégue, C. Ortiz, B. Sanyal, J. Fransson, and O. Eriksson, J. Phys.: Condens. Matter **21**, 335502 (2009).
27. X. Wang, Y. P. Chen, and D. D. Nolte, Opt. Express **16**, 22105 (2008).
28. R. M. A. Azzam and N. M. Bashara, *Ellipsometry and Polarized Light* (Amsterdam, 1977).
29. I. T. Kim and K. D. Kihm, Opt. Lett. **35**, 393 (2010).
30. K. S. Novoselov, D. Jiang, F. Schedin, T. J. Booth, V. V. Khotkevich, S. V. Morozov, and A. K. Geim, Proc. Natl. Acad. Sci. USA **102**, 10451 (2005).
31. Z. H. Ni, H. M. Wang, J. Kasim, H. M. Fan, T. Yu, Y. H. Wu, Y. P. Feng, and Z. X. Shen, Nano Lett. **7**, 2758 (2007).
32. P. B. Johnson and R. W. Christy, Phys. Rev. B **6**, 4370 (1972).

258

Queries

259
260 1. This query was generated by an automatic reference checking system. References [r24] could not be located in the
261 databases used by the system. While the references may be correct, we ask that you check them so we can provide
262 as many links to the referenced articles as possible.